PHYSICAL REVIEW D VOLUME 25, NUMBER 5 1 MARCH 1982

Development of ultrahigh-energy electromagnetic cascades in water and lead including the Landau-Pomeranchuk-Migdal effect

Todor Stanev and Ch. Vankov
Institute for Nuclear Research and Nuclear Energy, Sofia 1184, Bulgaria

R. E. Streitmatter
Laboratory for High Energy Astrophysics, NASA/Goddard Space Flight Center, Greenbelt, Maryland 20771

R. W. Ellsworth*
Department of Physics and Astronomy, University of Maryland, College Park, Maryland 20742

Theodore Bowen
Department of Physics, University of Arizona, Tucson, Arizona 85721
(Received 29 October 1981)

Cosmic-ray experiments are approaching energies where electromagnetic-cascade calculations must include the Landau-Pomeranchuk-Migdal (LPM) reduction in bremsstrahlung and pair-production cross sections. The LPM effect is already significant for cascades in Pb at 100 TeV and very important at 1000 TeV; for cascades of incident energy E_0 the LPM effect is significant if $E_0 >> E_{\rm LPM} = 61.5 L_{\rm cm}$ TeV, where $L_{\rm cm}$ is the radiation length in centimeters. Two totally independent Monte Carlo computer programs have been developed which, in approximation A, agree with each other and with Konishi, Misaki, and Fujimaki. One of these programs (by Stanev and Vankov) has been extended to include calculations of the lateral and angular distributions of cascade particles; the other (by Streitmatter, Ellsworth, and Bowen) has been utilized in a hybrid Monte Carlo and analytic method to calculate the longitudinal development in approximation B.

THE LANDAU-POMERANCHUK-MIGDAL (LPM) EFFECT

Landau and Pomeranchuk[1] showed with a semiclassical argument in 1953 that the bremsstrahlung and pair-production cross sections should decrease approximately as $E^{-1/2}$ when the incident energy E becomes sufficiently high in a dense medium, in contrast to the Bethe-Heitler (BH) energy-independent cross sections at lower energies. In 1956 Migdal[2] gave a quantum-mechanical treatment of the effect (which we denote as the LPM effect) upon which all subsequent workers have relied for the fundamental radiation and pair-production probabilities at ultrahigh energies. Although Greisen[3] pointed out the potential importance of the LPM effect in a 1965 review of air-shower studies, further developments came slowly because the LPM effect becomes important only at energies far above those availabe at accelerators and where cosmic-ray events are very rare.

As the attention of cosmic-ray physicists has moved toward energies $\gtrsim 10^3$ TeV ($=10^{15}$ eV) in emulsion chambers and $\gtrsim 10^8$ TeV in air showers, there has been a revival of interest in the LPM effect, both in experimental confirmation of the LPM radiation and pair-production cross sections and in including the LPM effect in electromagnetic-cascade calculations. Varfolomeev *et al.*[4] first reported qualitative evidence for the effect in a 1959 nuclear-emulsion study for bremsstrahlung in 10^{11}-to-10^{13}-eV cosmic-ray-produced electron-photon cascades. More recently Vafolomeev's group has quantitatively confirmed the LPM-predicted bremsstrahlung reduction in experiments with a 40-GeV electron beam at Serpukhov.[5] Comparisons were made of the intensity ratios of 20-to-80-MeV photons from Pb relative to Al and from W relative to C. In this energy range the predicted (and observed) intensity ratios from equal

thicknesses (measured in radiation lengths) of high-density and low-density materials fall in the range from 0.5 to 0.7. By observing the starting-point distributions of photon- and electron-initiated cascades with energies >1 TeV in emulsion chambers, Koss *et al.*[6] have found results consistent with the LPM cross sections.

By the time of the 1977 International Cosmic Ray Conference in Plovdiv, Bulgaria, three groups were developing Monte Carlo calculations of electromagnetic cascades which included the LPM effect.[7–10] However, although all began with the Migdal cross sections, no two calculations were in satisfactory agreement. In 1979 three of the authors (Streitmatter, Ellsworth, and Bowen) became interested in the LPM cascade problem and carried out a fourth independent Monte Carlo calculation,[11] both in "approximation A"[12] for comparison with the other groups, and a hybrid Monte Carlo and analytic calculation in " approximation B."[12] The results were found to be in excellent agreement with those of Misaki's group.[10] A one-year visit by another author (Stanev) to the United States allowed detailed comparisons which uncovered a programming error in the calculation of the Bulgarian group.[13] Because the cross checks of independent Monte Carlo programs proved to be very important, we agreed to publish together the combined results of the United States collaboration and the Bulgarian group.

QUALITATIVE EXPLANATION OF THE LPM EFFECT

For explanations of the LPM effect, the reader is referred not only to the original papers,[1,2] but also to a discussion by Nishimura.[14] The effect becomes important when the two electron momenta (initial and final electron momenta for radiation processes or e^+,e^- momenta for pair-production processes) become ultrarelativistic. Then the two electrons and a photon at a vertex have approximately zero mass, so the longitudinal momentum transfer $q_{||}$ can be very small. Conversely, the distance l along which the radiation process occurs becomes very long:

$$l \sim \frac{\hbar}{q_{||}} \sim \frac{2E_0(E_0-ck)}{(mc^2)^2}\frac{\hbar}{k} , \tag{1}$$

where E_0 is the initial electron energy, k is the photon momentum, and m is the electron mass. If the medium has sufficient density, other atoms may be encountered in traversing the distance l. These additional atoms cause multiple Coulomb scattering of the two electron waves introducing decoherence between the two states which reduces the result of the integration to obtain the transition matrix element.

The LPM suppression of the radiation matrix element becomes important when the rms multiple-Coulomb-scattering angle $\langle\theta_s^2\rangle^{1/2}$ becomes larger than the scattering angle θ_r due to the radiation process:

$$\langle\theta_s^2\rangle^{1/2} \gtrsim \theta_r \quad \text{(for LPM effect)} . \tag{2}$$

The multiple-Coulomb-scattering angle is

$$\langle\theta_s^2\rangle^{1/2} = (E_s/E_0)(l/L)^{1/2} , \tag{3}$$

where the scattering constant $E_s = mc^2(4\pi/\alpha)^{1/2} \cong 21$ MeV and L is the radiation length of the medium. The order of magnitude of the scattering angle due to the radiation process is

$$\theta_r \sim mc^2/E_0 . \tag{4}$$

Let the parameter s be defined by

$$s[\xi(s)]^{1/2} \equiv \theta_r/2\langle\theta_s^2\rangle^{1/2} \tag{5a}$$

$$= \left[\frac{mc^2}{2E_s}\right]\left[\frac{mc}{2\hbar}\right]^{1/2} \times \left[\frac{(mc^2)^2}{E_0(E_0-ck)}\frac{k}{mc}L\right]^{1/2} , \tag{5b}$$

where $\xi(s)$ is a logarithmic factor $\sim$ unity. Then the LPM suppression of the BH cross sections must be considered if

$$s \lesssim 1 \quad \text{(for LPM effect)} . \tag{6}$$

If the radiated photon energy kc is measured as a fraction u of the electron energy ($u \equiv kc/E_0$), then Eq. (5b) becomes

$$s = \left[\frac{1}{2}\left[\frac{\alpha}{4\pi}\right]^{1/2}\left[\frac{mc}{2\hbar}\right]^{1/2}\right]\left[\frac{mc^2}{E_0}\right]^{1/2}\left[\frac{u}{1-u}\right]^{1/2}\left[\frac{L}{\xi}\right]^{1/2} \quad \text{(bremsstrahlung)} , \tag{7}$$

where α is the fine-structure constant. The expression in the first square brackets in Eq. (7) has the numerical value 1.37×10^3 if L is in cm; this numerical constant often appears in LPM probabilities. For any

given electron energy $E_0 >> mc^2$, it can be seen from Eq. (7) that there is a region at the lower end of the radiated photon spectrum such that $s << 1$; hence the LPM effect always prevents an infrared catastrophe at the low end of the bremsstrahlung spectrum.

In pair production, Eq. (5b) can still be employed, but the energy E of one of the electrons is a fraction v of the incident photon energy ck_0 ($v \equiv E/ck_0$), so

$$\bar{s} = \left[\frac{1}{2}\left[\frac{\alpha}{4\pi}\right]^{1/2}\left[\frac{mc}{2\hbar}\right]^{1/2}\right]\left[\frac{mc^2}{ck_0}\right]^{1/2}\left[\frac{1}{v(1-v)}\right]^{1/2}\left[\frac{L}{\xi}\right]^{1/2} \quad \text{(pair production)} . \tag{8}$$

Since $1/v(1-v) \geq 4$, the LPM effect in pair production only becomes important at very high photon energies.

It is convenient to define an energy $E_{\rm LPM}$ which characterizes the energy above which the LPM effect is significant (i.e., $s << 1$ for $u \gtrsim \frac{1}{2}$ and $\bar{s} << 1$ for any v):

$$E_{\rm LPM} \equiv \left[\frac{4mc^2}{E_s}\right]^2\left[\frac{mc}{2\hbar}\right]Lmc^2 \tag{9a}$$

$$= [(8)(1.37\times 10^3)]^2 L_{\rm cm} mc^2 \tag{9b}$$

$$= 61.5 L_{\rm cm}\ \text{TeV} , \tag{9c}$$

where $L_{\rm cm}$ is the radiation length in centimeters. With this choice, the radiation length for bremsstrahlung and $\frac{4}{3}$ of the mean free path for pair production are given approximately (within $\sim 20\%$) by

$$L_{\rm LPM} \approx (E_0/E_{\rm LPM})^{1/2} L \quad (\text{when } E_0 >> E_{\rm LPM}) , \tag{10}$$

where L is the standard Bethe-Heitler radiation length for the medium. The factor $\frac{4}{3}$ for pair production should be compared with the familiar $\frac{7}{9}$ factor for $E_0 << E_{\rm LPM}$. The values of density, radiation length, and $E_{\rm LPM}$ for water and lead are listed in Table I.[15]

LPM RADIATION AND PAIR-PRODUCTION PROBABILITIES

In the quantitative theory of the LPM effect given by Migdal,[2] all radiation and pair-production cross sections are given as probabilities per BH radiation length, and all electron and photon energies (E and k in this section) are in units of mc^2, the electron rest energy. Many formulas are simplified by using the fractional radiated photon energy $u \equiv E/k_0$ and the fractional energy of one pair electron $v \equiv E/k_0$. If $F(E_0,u)du$ is the probability per radiation length of radiating a photon with fractional energy between u and $u+du$, then

$$F(E_0,u) = \xi(s)\{u^2 H(s) + 2[1+(1-u)^2]\phi(s)\}/3u \tag{11a}$$

$$= \xi(s)[u^2\psi(s) + (\tfrac{4}{3})(1-u)\phi(s)]/u \quad \text{(bremsstrahlung)} . \tag{11b}$$

If $G(k_0,v)dv$ is the probability per radiation length of pair production with one electron (say the e^-) with fractional energy between v and $v+dv$, then

TABLE I. Values of the density, radiation length, and $E_{\rm LPM}$ for water and lead.

	Water (H_2O)	Lead (Pb)
Density ρ (g/cm^3)	1.00	11.35
Radiation length (g/cm^2)	36.4	6.4
Radiation length $L_{\rm cm}$ (cm)	36.4	0.56
$E_{\rm LPM}$ (TeV)	2240	35

$$G(k,v)=\xi(\bar{s})\{H(\bar{s})+2[v^2+(1-v)^2]\phi(\bar{s})\}/3 \tag{12a}$$

$$=\xi(\bar{s})[\psi(\bar{s})-(\tfrac{4}{3})v(1-v)\phi(\bar{s})] \text{ (pair production)} . \tag{12b}$$

The functions $H(s)$, $\phi(s)$, and $\psi(s)$ are given by

$$H(s)\equiv 48s^2\left[\frac{\pi}{4}-\frac{1}{2}\int_0^\infty e^{-st}\frac{\sin(st)}{\sinh(t/2)}dt\right] \tag{13a}$$

$$=12\pi s^2-48s^3\sum_{j=0}^{\infty}[(j+s+\tfrac{1}{2})^2+s^2]^{-1} \tag{13b}$$

$$\cong\begin{cases}12\pi s^2 & (s<<1) \\ 1-0.029/s^4 & (s>>1) ,\end{cases} \tag{13c, 13d}$$

$$\phi(s)\equiv 12s^2\left[\int_0^\infty e^{-st}\coth(t/2)\sin(st)dt\right]-6\pi s^2 \tag{14a}$$

$$=6s-6\pi s^2+24s^3\sum_{j=1}^{\infty}[(j+s)^2+s^2]^{-1} \tag{14b}$$

$$\cong\begin{cases}6s(1-\pi s) & (s\le 0.01) \\ 1-\exp\{-6s[1+(3-\pi)s]+s^3/(0.623+0.796s+0.658s^2)\} & (0.01<s<2) \\ 1 & (s\ge 2) ,\end{cases} \tag{14c, 14d, 14e}$$

$$\psi(s)\equiv[H(s)+2\phi(s)]/3 \tag{15a}$$

$$\cong\begin{cases}4s & (s\le 0.01) \\ 1-\exp[-4s-8s^2/(1+3.936s+4.97s^2-0.05s^3+7.50s^4)] & (0.01<s<2) . \\ 1 & (s\ge 2)\end{cases} \tag{15b, 15c, 15d}$$

The approximate formulas in Eqs. (14c)–(14e) and (15b)–(15d) are accurate within 0.15% and were developed and employed by the the U.S. authors [Streitmatter, Ellsworth, and Bowen (SEB)] to reduce the computer time required to calculate the slowly convergent series in Eqs. (13b) and (14b). The series expression [Eqs. (13b) and (14b)] were given by Migdal,[16] and were employed by the Bulgarian authors [Stanev and Vankov (SV)] in performing their calculations.

The approximate expressions given by Migdal for the logarithmic factor $\xi(s)$ are

$$\xi(s)=\begin{cases}2 & (s\le s_1) \\ 1+(\ln s)/\ln s_1 & (s_1<s<1) , \\ 1 & (s\ge 1)\end{cases} \tag{16a, 16b, 16c}$$

where

$$s_1\equiv(Z^{1/3}/191)^2 , \tag{17}$$

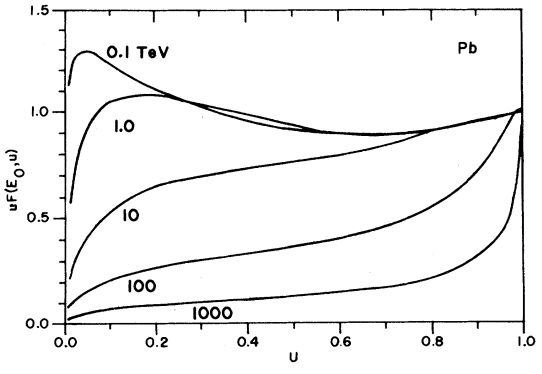

FIG. 1. Differential bremsstrahlung intensities per radiation length in Pb, $uF(E_0,u)$, for $E_0=0.1$, 1, 10, 100, 1000 TeV. The $E_0=0.1$ TeV curve is very close to the limiting curve for Bethe-Heitler cross sections; curves for higher E_0 cross this curve because of Migdal's approximation for $\xi(s)$ in Eqs. (16a)–(16c).

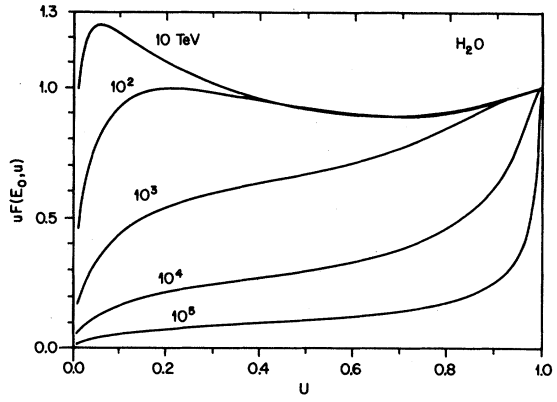

FIG. 3. Differential bremsstrahlung intensities per radiation length in H_2O, $uF(E_0,u)$, for $E_0=10$, 10^2, 10^3, 10^4, 10^5 TeV. The $E_0=10$ TeV curve is very close to the limiting curve for Bethe-Heitler cross sections; curves for higher E_0 cross this curve because of Migdal's approximations for $\xi(s)$ in Eqs. (16a)–(16c).

and Z is the atomic number of the scattering nuclei. Equations (7) and (8) for s and $\bar{s}$ require an iterative procedure for solution, since ξ appearing on the right-hand side is itself a function of s or $\bar{s}$. However, as ξ is only logarithmically dependent upon s, the following approximate formulas, accurate within 0.05%, allow ξ and s to be directly calculated without iteration:

$$s' \equiv \frac{1}{8}\left[\frac{E_{\rm LPM}}{E_0}\frac{u}{1-u}\right]^{1/2} \quad \text{(bremsstrahlung)}, \tag{18}$$

$$\bar{s}' \equiv \frac{1}{8}\left[\frac{E_{\rm LPM}}{k_0}\frac{1}{v(1-v)}\right]^{1/2} \quad \text{(pair production)}, \tag{19}$$

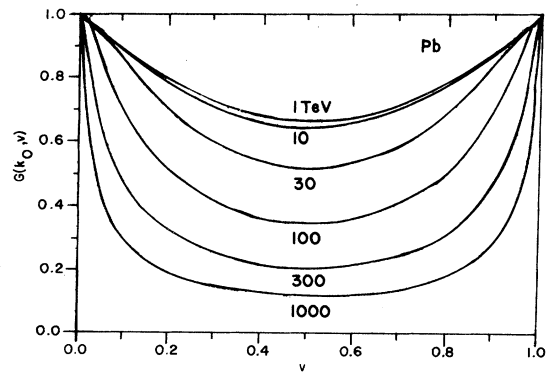

FIG. 2. Differential pair-production probabilities per radiation length in Pb, $G(k_0,v)$, for $k_0=1$, 10, 30, 100, 300, 1000 TeV. The $E_0=1$ TeV curve is very close to the limiting curve for Bethe-Heitler cross sections; curves for higher E_0 cross this curve because of Migdal's approximations for $\xi(s)$ in Eqs. (16a)–(16c).

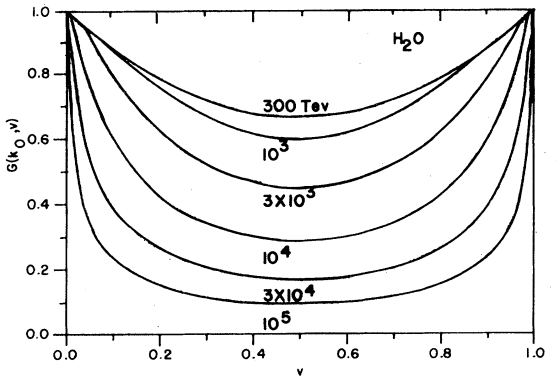

FIG. 4. Differential pair-production probabilities per radiation length in H_2O, $G(k_0,v)$, for $k_0=300$, 10^3, 3×10^3, 10^4, 3×10^4, 10^5 TeV. The $E_0=300$ TeV curve is very close to the limiting curve for Bethe-Heitler cross sections; curves for higher E_0 cross this curve because of Migdal's approximations for $\xi(s)$ in Eqs. (16a)–(16c).

$$h(s')\equiv(\ln s')/\ln(\sqrt{2}s_1)\ , \tag{20}$$

$$\xi(s')=\begin{cases} 2 \ \ (s'\leq\sqrt{2}s_1) & \text{(21a)} \\ 1+h-\dfrac{0.08(1-h)[1-(1-h)^2]}{\ln(\sqrt{2}s_1)} \ \ (\sqrt{2}s_1<s'<<1) & \text{(21b)} \\ 1 \ \ (s'\geq 1)\ , & \text{(21c)} \end{cases}$$

where s_1 is given by Eq. (17). Finally we obtain

$$s=s'/[\xi(s')]^{1/2}\ , \tag{22a}$$

$$\bar{s}=\bar{s}'/[\xi(\bar{s}')]^{1/2}\ . \tag{22b}$$

The approximation scheme of Eqs. (18)–(22) was developed and employed by SEB.

Figures 1 and 2 show the bremsstrahlung intensity distribution $uF(E_0,u)$ and the pair-production probability distribution $G(k_0,v)$ for Pb; Figs. 3 and 4 show the same distributions for H_2O. The authors have published tables of the corresponding integral distributions for Pb and H_2O.[17] It is clear from the figures that the radiation and pair-production probabilities are reduced by overall factors $\sim(E_{\rm LPM}/E_0)^{1/2}$ along with some change of shape. The complicated behavior of these distributions when $E_0>>E_{\rm LPM}$ necessitates Monte Carlo techniques for calculating the properties of electron-photon cascades.

For use in Monte Carlo calculations, tables of the integral distributions, such as those published by the authors,[17] were constructed. SEB computed these tables at factors of $10^{1/2}$ in energy from 10^9 to $10^{18.5}$ eV and in u,v from 10^{-5} to 1. SV chose factors of $10^{1/5}$ in energy from 10^{11} to 10^{17} eV, in u from 10^{-6} to 1, and in v from 10^{-4} to 1.

Recently, Bourdeau *et al.*[18] have reported LPM cascade calculations based upon a modification of Migdal's formulas which lower the bremsstrahlung and pair-production cross sections. As a result, the longitudinal development to cascade maximum occurs at greater depths in their calculations in comparison with this work.

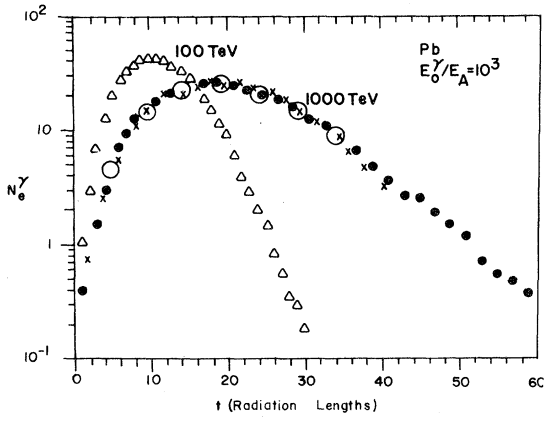

FIG. 5 Calculated number of electrons N_e^γ as a function of depth t in radiation lengths for photon-initiated cascades in Pb in approximation A including the LPM effect. $E_0^\gamma=10^2$, 10^3 TeV and $E_0^\gamma/E_A=10^3$. Δ,●: this work (by SEB), 100 cascades each; ×: this work (by SV), 200 cascades; ○: Konishi *et al.*, Ref. 10, 200 cascades.

LONGITUDINAL CASCADE DEVELOPMENT—APPROXIMATION A

The Monte Carlo program of SEB obtained by interpolation, from the table of integral probabilities, the appropriate mean-free path and the u or v corresponding to each random number choice of the integral probability. In order to generate results for comparison with Konishi *et al.*,[10] each electron and photon was followed in approximation A (Refs. 12 and 14) until its energy fell below $E_A=10^{-3}E_0^\gamma$, where E_0^γ is the initial photon energy. The number of electrons as a function of depth in Pb in photon-induced cascades was calculated for $E_0^\gamma=10$, 100, 1000 TeV. At 10 TeV, the LPM effect has negligible effect upon the longitudinal development of the cascade. Figure 5 shows the results at 100 and 1000 TeV. The results at 10^3 TeV are in excellent agreement with Konishi *et al.*[10] and with SV. The results of Ivanenko's group[8] at 10^3 TeV (not shown) have maxima at 10 to 12 radiation lengths and disagree with our results.

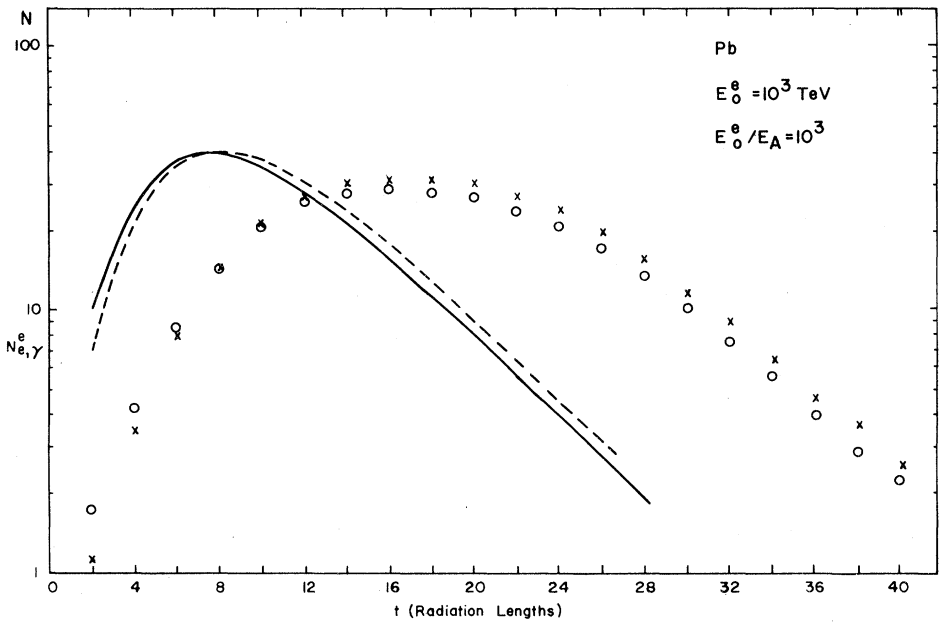

FIG. 6. Calculated numbers of electrons N_e^e and photons N_γ^e as a function of depth t in radiation lengths for electron-initiated cascades in Pb in approximation A including the LPM effect. $E_0^e = 10^3$ TeV. ○: N_e^e, ×: N_γ^e, this work (by SV), 200 cascades each; solid line: N_e^e, dashed line: N_γ^e, Ivanenko *et al.*, Ref. 8.

A different method was employed in the Monte Carlo program[19] of SV for the Bethe-Heitler (BH) case: A procedure proposed by Butcher and Messel[20] was used involving random selection and rejection of appropriately weighted terms whose sums comprise the desired distribution. Figure 6 shows the average longitudinal development of 200 electron-induced cascades in Pb at $E_0^e = 10^3$ TeV where all particles with $E > E_A = 10^{-3}\, E_0^e = 1$ TeV are included. The Ivanenko group results for electron-induced cascades[8] at this energy peak at about 8 radiation lengths in disagreement with our calculations.

In order to compare results with several earlier calculations, photon-initiated cascades were simulated with BH probabilities and with the more accurate LPM probabilities at initial energies $E_0^\gamma = 5$, 16, 50, and 150 TeV in Pb in which all secondaries were followed down to $E_A = 0.5$ TeV (see Fig. 7). The results with LPM cross sections are in excellent agreement with Astaf'ev *et al.*[7] The results using BH cross sections agree, as expected, with the Monte Carlo calculations of Adachi *et al.*[21] and with the analytic results of Misaki.[22] Results for cascades induced by photons in H_2O ($Z_{\text{eff}} \approx 7.23$) at $E_0^\gamma = 10^2$, 10^3, 10^4, and 5×10^4 TeV are shown in Fig. 8; all particles were followed until their energy fell below $E_A = 10^{-3} E_0^\gamma$. As expected, the LPM effect causes a slower cascade development with a lower, broader peak in the number of electrons for incident energies $E_0^\gamma >> E_{\text{LPM}} \approx 2.2 \times 10^3$ TeV in H_2O.

LONGITUDINAL CASCADE DEVELOPMENT—APPROXIMATION B

After verifying that the Monte Carlo program gave good agreement with others in approximation A, SEB modified their program to a hybrid Monte Carlo and analytic calculation in approximation B.[12,14] In the early part of the cascade, where the LPM effect is important, the development is traced by the Monte Carlo method. The subsequent cascade of each particle falling below $E_{\text{NKG}} << E_{\text{LPM}}$ is represented by the analytic Nishimura-Kamata-Greisen (NKG) formula[23] for the longitudinal development in approximation B. Below E_{NKG} Bethe-Heitler cross sections are an excellent approximation and the NKG formula provides a reasonable representation for the longitudinal distribution of the number of electrons. The final cascade distribution is obtained by summing all the NKG distributions, each with initial energy E and depth corresponding to a particle generated by the Monte

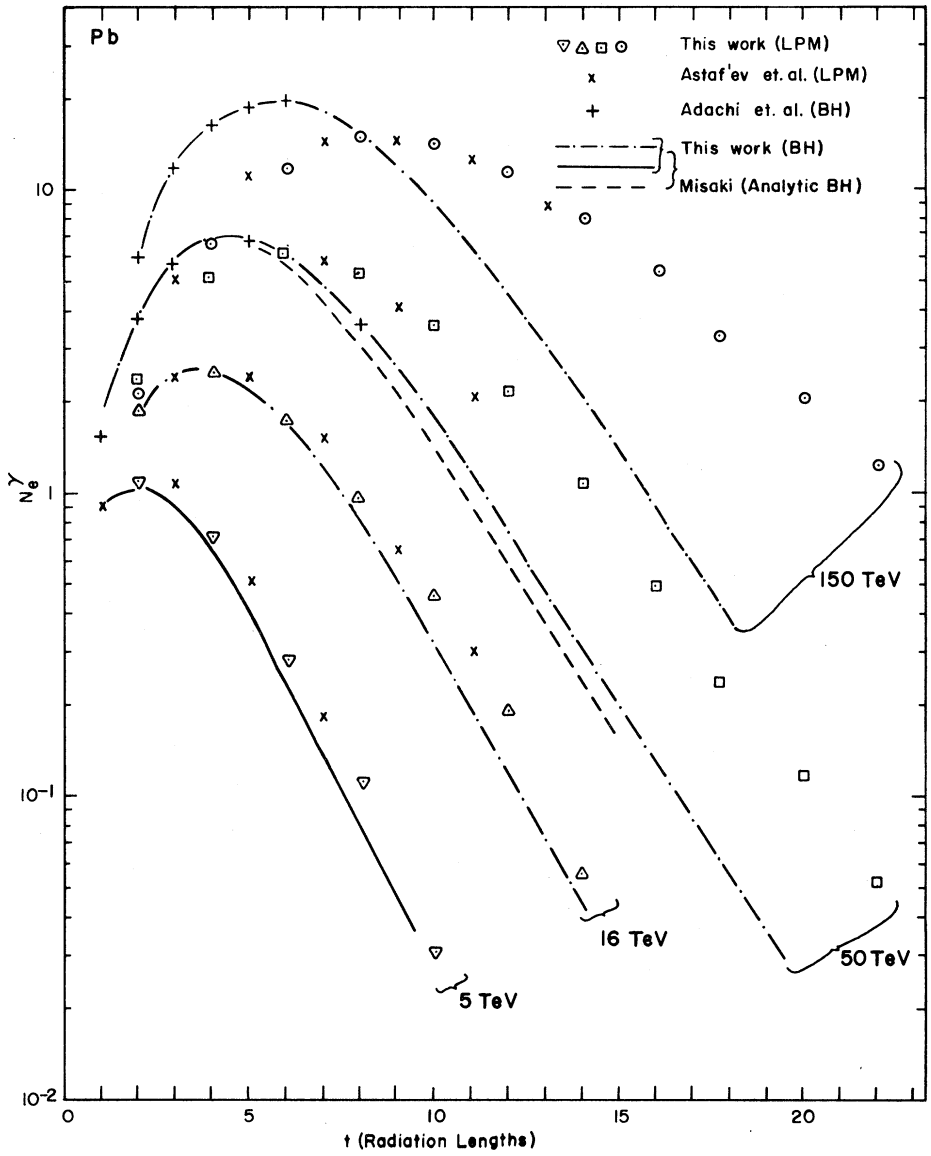

FIG. 7. Calculated number of electrons N_e^γ as a function of depth t in radiation lengths for photon-initiated cascades in Pb in approximation A. E_0^γ=5, 16, 50, 150 TeV, E_A=0.5 TeV. The results including LPM effect are shown as ∇ (1000 cascades), Δ, □, ○ (200 cascades each): this work (by SV); ×: Astaf'ev *et al.*, Ref. 7, 500 cascades each energy (for clarity, some points not shown). The results assuming Bethe-Heitler cross sections are shown as (a) solid curve: this work (by SV), Monte Carlo, 200 cascades and Misaki, Ref. 22, analytic; (b) dot-dashed curve: this work (by SV), Monte Carlo, 200 cascades each energy; (c) dashed curve: Misaki, Ref. 22, analytic; (d) +: Adachi *et al.*, Ref. 21, Monte Carlo, 500 cascades each energy (for clarity, some points not shown).

Carlo program with $E < E_{\mathrm{NKG}}$.

The NKG distribution[23] for the number of electrons $N(E_0,t)$ at depth t (measured in radiation lengths) in a cascade with initial energy E_0 was taken in the form

$$N(E_0,t) \cong (0.31/\beta_0^{1/2}) \times \exp\{t[1-(\tfrac{3}{2})\ln s]\}\ , \tag{23}$$

$$\beta_0 \equiv \ln\frac{E_0}{\epsilon_0}\ , \tag{24}$$

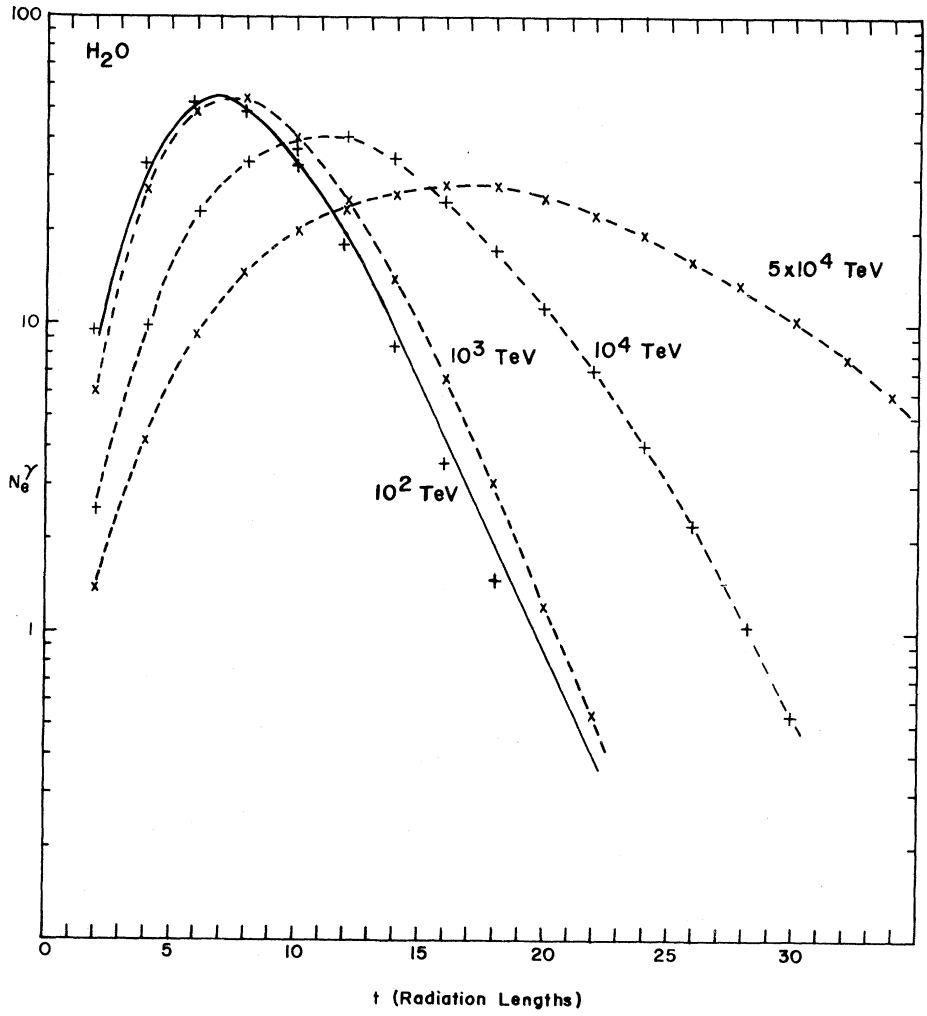

FIG. 8. Calculated number of electrons N_e^γ as a function of depth t in radiation lengths for photon-initiated cascades in H_2O in approximation A including the LPM effect: $E_0^\gamma = 10^2$, 10^3, 10^4, 5×10^4 TeV, $E_0^\gamma/E_A = 10^3$, this work (by SV), 140 cascades at 10^2 TeV, 200 cascades each at 10^3 and 10^4 TeV, 100 cascades at 5×10^4 TeV. Solid curve: Misaki, Ref. 22, analytic calculation using Bethe-Heitler cross sections. Dashed curves drawn to guide the eye.

$$s \equiv 3t/(t+2\beta_0)\,, \tag{25}$$

where ϵ_0 is the critical energy and s is the shower age parameter. ($\epsilon_0 = 73$ MeV for water and 7.6 MeV for Pb were assumed.)

It was found that the hybrid method requires following only a small number of cascades since much of the averaging over fluctuations is included in the individual analytic NKG distributions. This is illustrated in Fig. 9, where the results at 10^3 TeV in Pb are shown for five calculations, three of which show single cascades, one shows the average of two cascades, and one shows the average of 100 cascades.

For Pb, 1 TeV was chosen for $E_{\rm NKG}$. Figures 10 and 11 show the hybrid calculation results for 100 photon-initiated cascades at 100 and 1000 TeV. Also shown for comparison are the curves given by the NKG approximation B formula [Eqs. (23)–(25)] if the LPM effect is neglected. The result are in excellent agreement with independent calculations by Fujimaki and Misaki[24] and by Kokoulin and Petrukhin.[24]

Calculations were also carried out for photon-initiated cascades in water, where 100 TeV was chosen for $E_{\rm NKG}$. Figures 12, 13, and 14 show the results at 10^3, 10^4, and 10^5 TeV along with NKG approximation B curves neglecting the LPM effect.

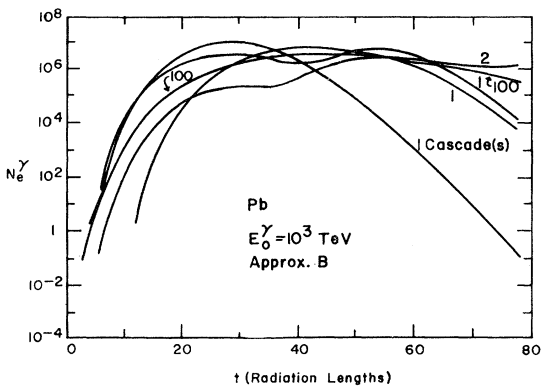

FIG. 9. Examples of hybrid Monte Carlo—analytic simulated LPM cascades in approximation B initiated by 10^3-TeV photons in Pb, this work (by SEB). Each curve is labeled with the number of cascades employed.

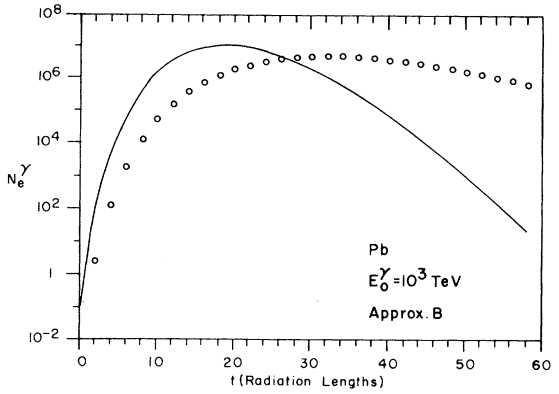

FIG. 11. Hybrid Monte Carlo—analytic approximation B calculation of the number of electrons N_e^γ as a function of depth t in radiation lengths for 1000-TeV photon-initiated cascades in Pb; ○: LPM effect included, this work (by SEB), 100 cascades; solid curve: NKG formula based upon Bethe-Heitler cross sections.

ANGULAR AND LATERAL DISTRIBUTIONS OF CASCADE ELECTRONS

The modification of radiation and pair-production probabilities by the LPM effect also affects the angular and lateral distributions of the secondary shower particles. Since the LPM distributions are more sharply peaked then the corresponding BH distributions (see Figs. 1 and 2, or 3 and 4), the LPM effect causes an enhancement of the proportion of very energetic secondaries in the cascade. These energetic particles suffer less multiple Coulomb scattering.

The angular and lateral distributions were obtained from Monte Carlo calculations by SV in approximation A for cascades of primary energy $E_0^{\gamma,e}$, and following all particles with energy $E > E_A << E_0^{\gamma,e}$. The production of bremsstrahlung photons and pair electrons was assumed to be exactly forward relative to the primary particle of the collision. The angular and lateral position of each secondary was computed at depths of 2 radiation lengths taking into account multiple Coulomb

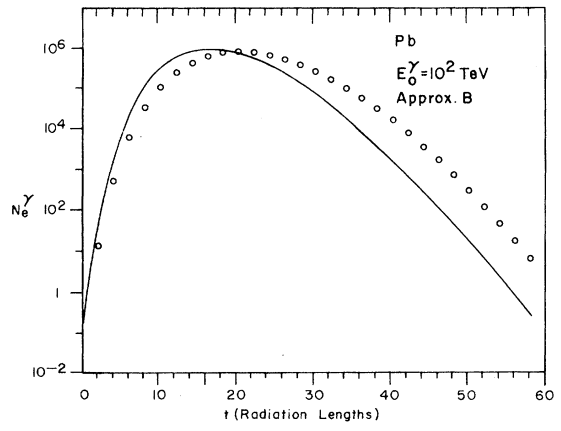

FIG. 10. Hybrid Monte Carlo—analytic approximation B calculation of the number of electrons N_e^γ as a function of depth t in radiation lengths for 100-TeV photon-initiated cascades in Pb; ○: LPM effect included, this work (by SEB), 100 cascades; solid curve: NKG formula based upon Bethe-Heitler cross sections.

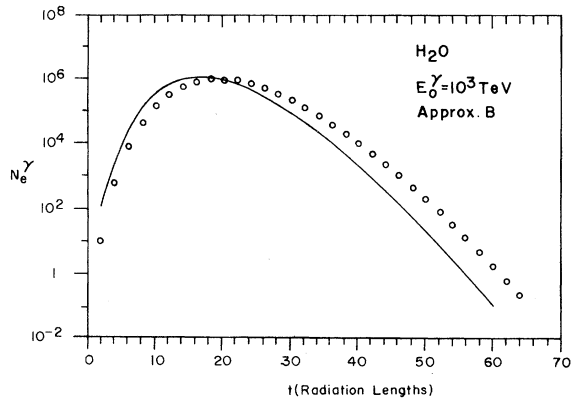

FIG. 12. Hybrid Monte Carlo—analytic approximation B calculation of the number of electrons N_e^γ as a function of depth t in radiation lengths for 10^3-TeV photon-initiated cascades in H_2O; ○: LPM effect included, this work (by SEB), 15 cascades; solid curve: NKG formula based upon Bethe-Heitler cross sections.

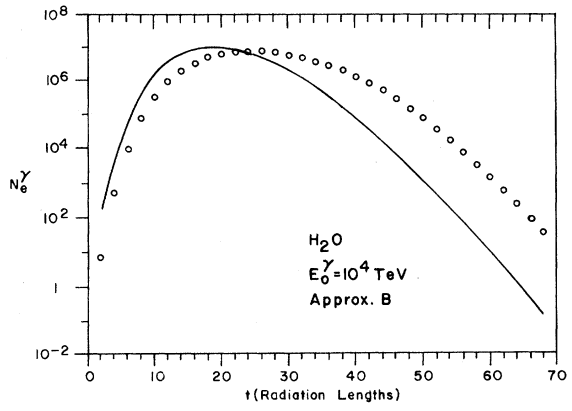

FIG. 13. Hybrid Monte Carlo—analytic approximation B calculation of the number of electrons N_e^γ as a function of depth t in radiation lengths for 10^4-TeV photon-initiated cascades in H_2O; ○: LPM effect included, this work (by SEB), 20 cascades; solid curve: NKG formula based upon Bethe-Heitler cross sections.

scattering and geometry. Multiple scattering was computed[19] using the first two terms of the Molière distribution[25] as parametrized by Bethe[26]; the first term is a Gaussian and the second term corresponds to large-angle single scattering.

Figure 15 shows the electron mean-square angle $\langle\theta^2\rangle$ and mean-square lateral position $\langle R^2\rangle$ weighted by the factor $(E_A/E_s)^2$, where $E_s \cong 21$

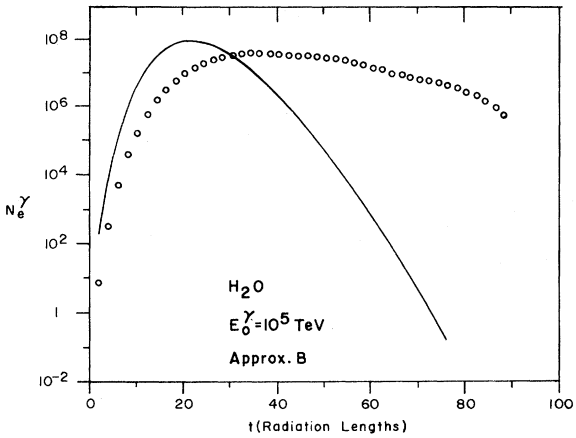

FIG. 14. Hybrid Monte Carlo—analytic approximation B calculation of the number of electrons N_e^γ as a function of depth t in radiation lengths for 10^5-TeV photon-initiated cascades in H_2O; ○: LPM effect included, this work (by SEB), 25 cascades; solid curve: NKG formula based upon Bethe-Heitler cross sections.

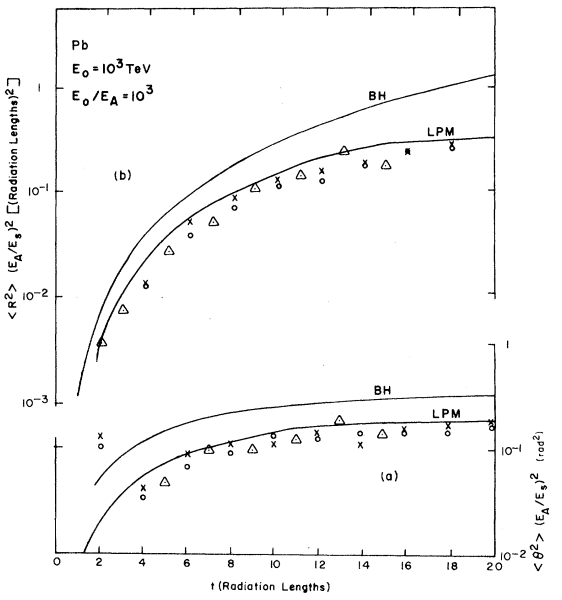

FIG. 15. (a) Normalized mean-square angle $\langle\theta^2\rangle(E_A/E_s)^2$ in (radians)^2 and (b) normalized mean-square lateral position $\langle R^2\rangle(E_A/E_s)^2$ in (radiation lengths)^2 of the cascade electrons as a function of depth t in radiation lengths in Pb for primary energy $E_0 = 10^3$ TeV, $E_0/E_A = 10^3$. ○: photon primary, ×: Electron primary, this work (by SV), 200 cascades each; Δ: photon primary, Konishi *et al.*, Ref. 10, 200 cascades (some points omitted for clarity). The curves show the analytic results for photon primaries of Misaki, Ref. 27, assuming Bethe-Heitler cross sections and of Fujimaki and Misaki, Ref. 28, for LPM cross sections.

MeV, as a function of depth for photon- and electron-initiated 10^3-TeV cascades in Pb including all electrons with $E > E_A = 1$ TeV. For comparison, curves obtained using analytic theory for BH cross sections by Misaki[27] and using numerical calculations for LPM cross sections by Fujimaki and Misaki[28] are also shown in Fig 15. For depths $t \gtrsim 10$ radiation lengths, which includes the region of the cascade maximum (see Fig. 6) $\langle\theta^2\rangle(E_A/E_s)^2 \approx 0.12$ compared to ≈ 0.25 without the LPM effect.[27] The mean-square lateral position $\langle R^2\rangle(E_A/E_s)^2$ is reduced by a larger factor by the LPM effect, indicating the lower-energy electrons tend to originate closer to the sampled layer. Results shown from Konishi *et al.*[10] for photon-induced cascades are in good agreement. The results in Fig. 15 indicate that the nature of the primary particle (photon or electron) has very little effect upon $\langle\theta^2\rangle$ or $\langle R^2\rangle$.

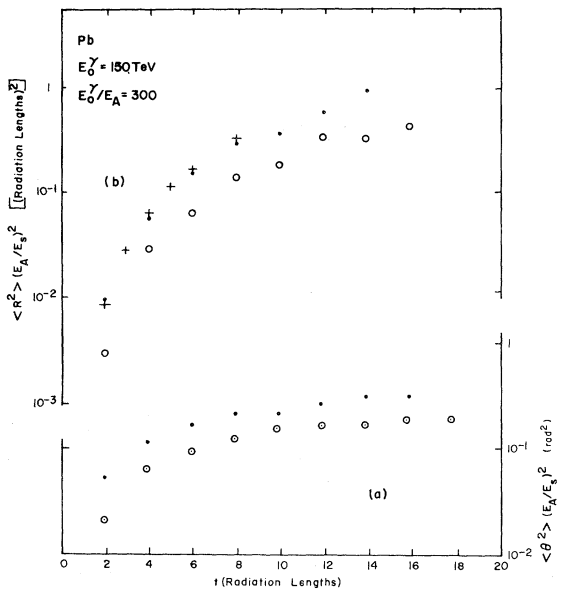

FIG. 16. Normalized mean-square angle $\langle\theta^2\rangle(E_A/E_s)^2$ in (radians)^2 and (b) normalized mean-square lateral position $\langle R^2\rangle(E_A/E_s)^2$ in (radiation lengths)^2 of the cascade electrons as a function of depth t in radiation lengths in Pb for primary photon energy $E_0^\gamma=150$ TeV, $E_0^\gamma/E_A=300$. ○: including LPM effect, ●: assuming Bethe-Heitler cross sections, this work (by SV), 200 cascades each; +: Adachi *et al.*, Ref. 21, 500 cascades.

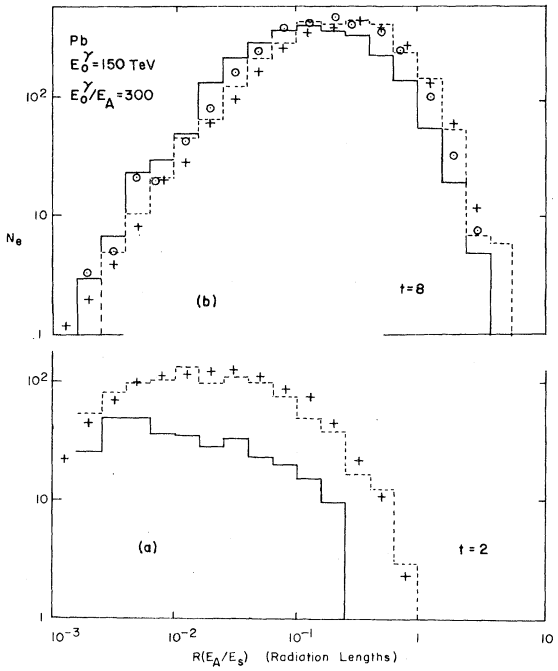

FIG. 17. Number of electrons versus normalized distance $R(E_A/E_s)$ from the cascade axis for photon primary energy $E_0^\gamma=150$ TeV, $E_0^\gamma/E_A=300$ in Pb (a) at $t=2$ radiation lengths depth and (b) at 8 radiation lengths depth. Solid lines: including LPM effect; dashed lines: Bethe-Heitler cross sections, this work (by SV), 200 cascades. ○: including LPM effect, Astaf'ev *et al.*, Ref. 7, 500 cascades (ordinates divided by 2.5); ×: Bethe-Heitler cross sections, Adachi *et al.*, Ref. 21, 500 cascades (ordinates divided by 2.5). Each histogram entry represents the total number of electrons in the interval R_i to $R_i(10^{0.2})$ from 200 cascades; Refs. 7 and 21 gave similar plots, but normalized to 500 cascades.

Figure 16 shows $\langle\theta^2\rangle(E_A/E_s)^2$ and $\langle R^2\rangle(E_A/E_s)^2$ as a function of depth for photon-initiated 150-TeV cascades of $E>E_A=0.5$ TeV electrons in Pb for comparison with BH cross sections and with Adachi *et al.*[21] For these 200 simulated cascades, Fig. 17 shows the distribution of normalized lateral position $R(E_A/E_s)$ at depths $t=2$ and 8 radiation lengths. When the LPM effect is included, the maximum lateral position at which electrons are found decreases appreciably.

Results for the mean-square angle and lateral position in water are shown in Fig. 18 for $E_0^\gamma=10^3$ and 10^4 TeV including all electrons with $E>E_A=10^{-3}E_0^\gamma$. The solid curve in Fig. 18 was calculated from the analytic theory based upon BH cross sections.[27] Since Table I indicates $E_{\rm LPM}\cong 2.24\times 10^3$ TeV for water, the results of Fig. 18 confirm that the LPM effect becomes important for cascade properties when $E_0>>E_{\rm LPM}$; qualitatively the changes caused by the LPM effect are very similar in H_2O and Pb.

CONCLUSIONS

We have given a number of examples of simulated cascade development in Pb and H_2O for primary energies $E_0>>E_{\rm LPM}$ where the LPM effect becomes important. Qualitatively, the effect should be similar in any material as a function of $E_0/E_{\rm LPM}$; the cascade properties do not scale exactly with this parameter because of logarithmic factors dependent upon the atomic number Z of the medium. It is hoped that the results will guide the reader in designing experiments and planning further calculations. For the analysis of specific high-energy-cascade events, the experimenter will have to simulate cascades for the materials present in his experimental situation; it is hoped that our

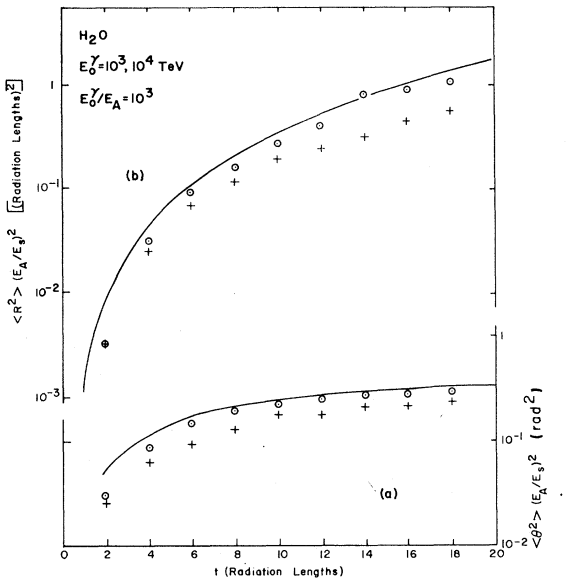

FIG. 18. Normalized mean-square angle $\langle\theta^2\rangle(E_A/E_s)^2$ in (radians)^2 and (b) normalized mean-square lateral position $\langle R^2\rangle(E_A/E_s)^2$ in (radiation lengths)^2 of the cascade electrons as a function of depth t in radiation lengths in H_2O for primary photon energies $E\gamma_0=10^3$, 10^4 TeV, $E\gamma_0/E_A=10^3$. $\circ$: $E\gamma_0=10^3$ TeV, $+$: $E\gamma_0=10^4$ TeV, including LPM effect, this work (by SV), 200 cascades each energy. Solid curve: analytic results assuming Bethe-Heitler cross sections, Misaki, Ref. 27.

results will provide convenient comparisons in tests for proper operation of his Monte Carlo routines.

At high energies where the LPM effect is important, the longitudinal cascade development will be very similar to a hadronic-electromagnetic cascade. Separation of electron- and photon-initiated cascades from hadron-initiated cascades by cascade characteristics will become less effective.

Air showers typically originate in the upper atmosphere where the pressure is on the order of 0.1 atm. At this pressure, $E_{\rm LPM}=1.8\times10^{19}$ eV; as primary cosmic-ray energies exceed 10^{20} eV, the LPM effect will cause air showers to develop more gradually. At sufficiently high energy, air showers will deposit only a small fraction of their energy before reaching sea level; this effect requires further study.

ACKNOWLEDGMENTS

This work was assisted by National Science Foundation (NSF) Grant No. INT78-17132 to one of the authors (T.S.), NSF Grants Nos. PHY77-01438 and PHY79-08641, and the University of Maryland Computer Science Center. While this work was in progress, one of the authors (T.S.) enjoyed the hospitality of cosmic-ray groups at the University of Maryland, University of Utah, and Bartol Research Foundation/University of Delaware during a one-year visit to the U.S. SEB wish to express their appreciation to Dr. A. Misaki for helpful discussions during his U.S. trip; a portion of the work by two of them (R.E.S. and T.B.) was performed while NASA/National Academy of Sciences Research Associates at Goddard Space Flight Center.

*Now at Department of Physics, George Mason University, Fairfax, Virginia 22030.

[1]L. Landau and I. Pomeranchuk, Dok. Akad. Nauk SSSR 92, 535, (1953); 92, 735 (1953).

[2]A. B. Migdal, Phys. Rev. 103, 1811 (1956); Zh. Eksp. Teor. Fiz. 32, 633 (1957) [Sov. Phys.—JETP 5, 527 (1957)].

[3]K. Greisen, in *Proceedings of the Ninth International Cosmic Ray Conference, London, 1965* (Institute of Physics and the Physical Society, London, 1966), Vol. 2, p. 609.

[4]A. A. Varfolomeev, R. I. Gerasimova, I. I. Gurevich, L. A. Makar'ina, A. S. Romantseva, and S. A. Chueva, Zh. Eksp. Teor. Fiz. 38, 33 (1960) [Sov. Phys.—JETP 11, 23 (1960)].

[5]A. A. Varfolomeev, V. I. Glebov, E. I. Denisov, A. M. Frolov, and A. S. Khlebnikov, Zh. Eksp. Teor. Fiz. 69, 429 (1975) [Sov. Phys.—JETP 42, 218 (1976)].

[6]T. A. Koss, J. J. Lord, R. J. Wilkes, and T. Stanev, *17th International Cosmic Ray Conference, Paris, 1981, Conference Papers* (Centre d'Etudes Nucleaires, Saclay, 1981), Vol. 5, p. 230, and (private communication).

[7]V. A. Astaf'ev, A. K. Bakhtadze, A. A. Belyaev, N. M. Gerasimova, R. M. Golynskaya, V. V. Guzhavin, E. I. Daibog, I. P. Ivanenko, B. L. Kanevskii, V. V. Makarov, R. A. Mukhamedshin, L. N. Osipova, T. M. Roganova, and G. F. Fedorova, Izv. Akad. Nauk

SSSR, Ser. Fiz. 40, 969 (1976) [Bull. Acad. Sci. USSR, Phys. Ser. 40, 79 (1976)]. The ordinate N_e of Fig. 1 of this paper must be corrected by multiplying by a factor of 0.1.

[8]I. P. Ivanenko, B. L. Kanevsky, A. A. Kirillov, T. S. Lim, A. A. Belyaev, Yu. G. Lyutov, and T. M. Roganova, in *Proceedings of the Fifteenth International Conference on Cosmic Rays, Plovdiv,* 1977, edited by B. L. Betev (Bulgarian Academy of Science, Sofia, 1977), Vol. 7, p. 292. I. P. Ivanenko, A. A. Kirillov, and Yu. G. Lyutov, in *Sixteenth International Cosmic Ray Conference, Kyoto, 1979, Conference Papers* (Institute of Cosmic Ray Research, Univ. of Tokyo, Tokyo, 1979), Vol. 9, p. 247. Although these papers, where $E_0 \geq 10^3$ TeV, and Ref. 7, where $E_0 \leq 150$ TeV share several authors, the results do not fit a smooth extrapolation between energy ranges. For example, at $E\gamma = 150$ TeV, $E\gamma/E_A = 300$ in Ref. 7, the LPM cascade maximum occurs at $t = 8$ radiation lengths (in agreement with us). However, in Ref. 8 at $E\gamma = 1000$ TeV, $E\gamma/E_A = 1000$ the maximum is at about $t = 9$ radiation lengths, whereas this depth should have substantially increased for two reasons: (a) At higher $E\gamma$, the greater LPM effect should increase the depth of cascade maximum and (b) at higher $E\gamma/E_A$ the depth of cascade maximum should be increased independent of the LPM effect.

[9]T. Stanev, Ch. Vankov, and T. Vodenicharova, in *Proceedings of the Fifteenth International Conference on Cosmic Rays Plovdiv, 1977* (Ref. 8), Vol. 7, p. 256.

[10]E. Konishi, A. Misaki, and N. Fujimaki, Nuovo Cimento 44A, 509 (1978).

[11]R. W. Ellsworth, R. E. Streitmatter, and T. Bowen, in *Sixteenth International Cosmic Ray Conference, Kyoto, 1979, Conference Papers* (Ref. 8), Vol. 7, p. 55; R. E. Streitmatter, R. W. Ellsworth, and T. Bowen, in *Proceedings of the 1979 DUMAND Summer Workshop, Khaborovsk and Lake Baikal, USSR,* edited by J. Learned (Hawaii DUMAND Center, Univ. of Hawaii, Honolulu, 1980), p. 53.

[12]B. Rossi, *High Energy Particles* (Prentice-Hall, Englewood Cliffs, N. J., 1952), pp. 214–298.

[13]An error in computer programming invalidates the initial results reported by T. Stanev and Ch. Vankov, in *Sixteenth International Cosmic Ray Conference, Kyoto, 1979, Conference Papers* (Ref. 8), Vol. 7, p. 47.

[14]J. Nishimura, in *Handbuch der Phyzik,* edited by S. Flügge (Springer, Berlin, 1967), Vol. 46, pt. 2.

[15]O. I. Dovzhenko and A. A. Pomanskii, Zh. Eksp. Teor. Fiz. 45, 268 (1963) [Sov. Phys.—JETP 18, 187 (1964)]; Y. S. Tsai, Rev. Mod. Phys. 46, 815 (1974).

[16]There are several typographical errors in the formulas given in Migdal's original papers (Ref. 2); most can be recognized by comparing the Phys. Rev. and JETP publications. Konishi *et al.*, Ref. 10, also repeat one of these errors in their Eq. (3); however, they have used the correct formula in their calculations (private communication).

[17]T. Bowen, R. W. Ellsworth, T. Stanev, R. E. Streitmatter, and Ch. Vankov, At. Data Nucl. Data Tables 24, 495 (1979).

[18]M. F. Bordeau, J. N. Capdevielle, and J. Procureur, *17th International Cosmic Ray Conference, Paris, 1981, Conference Papers* (Ref. 6), Vol. 5, p. 170.

[19]T. Stanev and Ch. Vankov, Comput. Phys. Commun. 16, 363 (1979).

[20]J. C. Butcher and H. Messel, Phys. Rev. 112, 2096 (1958); Nucl. Phys. 20, 15 (1960).

[21]A. Adachi, Y. Fujimoto, N. Ogita, S. Takagi, and A. Ueda, Prog. Theor. Phys. Suppl. 32, 154 (1964).

[22]A. Misaki, Prog. Theor. Phys. 31, 717 (1964).

[23]K. Greisen, in *Progress in Cosmic Ray Physics,* edited by J. G. Wilson (North-Holland, Amsterdam, 1956), Vol. 3, p. 3.

[24]N. Fujimaki and A. Misaki, in *Sixteenth International Cosmic Ray Conference, Kyoto, 1979, Conference Papers* (Ref. 8), Vol. 13, p. 51; R. P. Kokoulin and A. A. Petrukhin, *ibid.* Vol. 7, p. 30, and Yad. Fiz. 32, 1030 (1980) [Sov. J. Nucl. Phys. 32, 532 (1980)].

[25]G. Molière, Z. Naturforsch. 3a, 78 (1948).

[26]H. A. Bethe, Phys. Rev. 89, 1256 (1953).

[27]A. Misaki, Prog. Theor. Phys. Suppl. 32, 82 (1964).

[28]N. Fujimaki and A. Misaki, *17th International Cosmic Ray Conference., Paris, 1981, Conference Papers* (Ref. 6), Vol. 5, p. 162.